Available online at www.sciencedirect.com

ScienceDirect

Soils and Foundations 57 (2017) 301–314

www.elsevier.com/locate/sandf

Interface shear strength between geosynthetic clay liner and covering soil on the embankment of an irrigation pond and stability evaluation of its widened sections

Motoyuki Suzuki [a,*], Atsushi Koyama [b], Yoshifumi Kochi [c], Tomoko Urabe [d]

[a] *Graduate School of Sciences and Technology for Innovation, Yamaguchi University, 2-16-1, Tokiwadai, Ube, Yamaguchi 755-8611, Japan*
[b] *Graduate School of Science and Engineering, Yamaguchi University, 2-16-1, Tokiwadai, Ube, Yamaguchi 755-8611, Japan*
[c] *K's Lab. Co., 3533-4, Osaba, Yamaguchi, Yamaguchi 753-1212, Japan*
[d] *Volclay Japan Co., Ltd., 3-1-9, Shimbashi, Minato-ku, Tokyo 105-0004, Japan*

Received 30 June 2015; received in revised form 26 December 2016; accepted 15 January 2017
Available online 28 April 2017

Abstract

Geosynthetic clay liners (GCLs) are typically used for widening sections of an embankment. They are also used as low permeability liners to minimize water leakage from reservoirs such as irrigation ponds. However, few investigations have been carried out on the specific properties of GCLs, such as granulated bentonite sandwiched between geotextiles, their internal shear strength, and the shear strength at the interface between a GCL and an embankment body. In this study, a series of direct box shear tests were performed to determine the shear strength properties of bentonite and compacted soils as well as at the interface between a GCL and bentonite or compacted soil. In addition, a series of field-loading tests were conducted to investigate the failure behaviour of an embankment body containing a GCL when changes in the water content of the bentonite of the GCL in a real embankment occur. Furthermore, the stability of widened embankment bodies that incorporated GCLs were evaluated. The main conclusions of this study are as follows: (1) The shear strength of the interface between the covering soil and geotextiles varied according to the soil type, geotextile type, and the submergence period, (2) the maximum safety factor was observed at the interface between decomposed granite soil and the geotextiles, while the minimum safety factor was observed at the interface between the bentonite and the geotextiles, and (3) the influence of GCLs on the instability of a widened embankment was extremely small.

Keywords: Embankment; Geosynthetic clay liner; Bentonite; Interface shear strength; Field test; Slope stability (**IGC**: D06/E06/H04)

1. Introduction

There are approximately 210,000 irrigation ponds in Japan, some of which have significantly deteriorated over their life span. For instance, the stability of an embankment body diminishes when water leaks or deformation of the embankment occurs. Hence, it is essential to repair the damaged portions affected by deterioration to prevent the failure of irrigation ponds. Generally, repairs involve the use of high-quality clay as a water barrier in irrigation ponds. However, as the banking or covering soil in the embankment is subject to erosion, it is considered difficult to replace the soil lost due to erosion. Recently, a method that involves the widening of a section of the previous embankment over a geosynthetic clay liner (GCL; Fig. 1) has been developed in the field of agricultural civil engineering (Natsuka et al., 1993; Bouazza, 2002; Hara et al., 2009).

Peer review under responsibility of The Japanese Geotechnical Society.
* Corresponding author. Fax: +81 836 85 9301.
E-mail address: msuzuki@yamaguchi-u.ac.jp (M. Suzuki).

http://dx.doi.org/10.1016/j.sandf.2017.03.007
0038-0806/

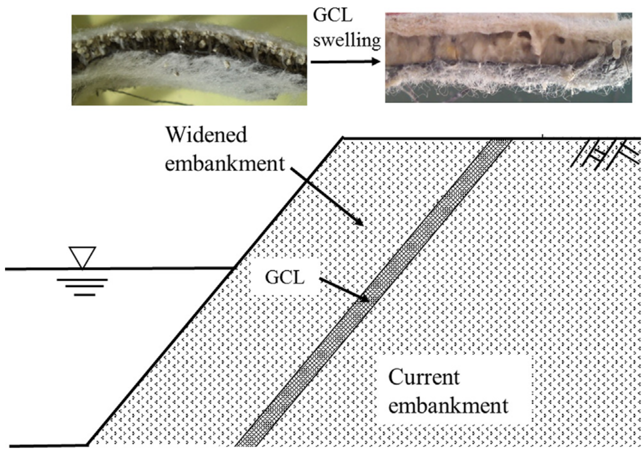

Fig. 1. An embankment widened across a GCL.

GCLs consist of layers of bentonite sandwiched between woven and non-woven geotextiles using needle-punches (Daniel and Koerner, 2007). They prevent leaks in irrigation ponds by permitting the infiltration of water, which causes the bentonite to swell. Several studies have verified the engineering application of bentonite for solving advanced environmental problems (Komine and Ogata, 1994; Kodaka and Teramoto, 2009). In addition, GCLs containing expansive clay minerals such as montmorillonite have also been used in waste disposal sites; this confirms their chemical durability and their performance as a long-term barrier (Malusis and Shackelford, 2002; Lee and Shackelford, 2005; Katsumi et al., 2008).

The internal shear strength of needle-punched GCLs has been determined and their resistance against sliding has been demonstrated (Gilbert et al., 1996; Stark and Eid, 1996; Fox et al., 1998a; Zornberg et al., 2005; Fox, 2010; Bacas et al., 2013; Fox et al., 2015; Fox and Stark, 2015). It was proposed that the strength of a GCL depends on the type of material used for the geotextiles as well as the connections between the needle-punch and the geotextiles. Furthermore, the peak and residual shear strengths of reinforced GCLs were influenced by the rate of shear displacement due to excess pore pressures on bentonite and the pull-out or rupture of the needle-punched fibres.

Moreover, the peak shear strengths of hydrated reinforced GCLs were lower than those of dry reinforced GCLs (Bacas et al., 2013). While the time required to achieve the complete hydration of a GCL depends on the drainage conditions, it generally decreases with increased normal stress (Gilbert et al., 1996; Fox and Stark, 2015). A few studies on the interface shear strength between GCLs and geomembranes (GM) have been carried out, and the results demonstrated that the interfaces typically have low shear strengths due to the extrusion of bentonite from the hydrated GCL (Seo et al., 2007; Vukelic et al., 2008; Chen et al., 2010; Saito et al., 2013). Further, Athanassopoulos and Yuan (2011) reported a correlation between the peel and internal shear strengths of a GCL; they concluded that the peak internal shear strength was a function of peel strength in the hydrated needle-punched GCL. In addition, Hurst and Rowe (2006) demonstrated that the average bonding peel strength of a needle-punched structure was not affected in a hydrated GCL under an applied normal stress of 14 kPa for a period of up to 15 days. It was observed that the internal shear strength of a GCL increased due to needle-punching (Zornberg et al., 2005). Thus, it would seem evident that the needle-punched structure improved the internal shear strength of the GCLs. However, a study by Fox (2010) indicated that the internal shear strength of GCLs also depends on the product type. As mentioned above, previous studies have demonstrated the characteristics of the internal shear strength and swelling behaviour of GCLs. Nevertheless, to evaluate the stability of embankments over GCLs, it is necessary to understand the characteristics of the shear strength of the interface of each soil layer. Direct box shear tests have been conducted in several previous studies to determine the behaviour of the interface between soil and woven or non-woven geotextiles (Lee and Manjunath, 2000; Goodhue et al., 2001; Anubhav and Basudhar, 2010; Khoury et al., 2011). Goodhue et al. (2001) have highlighted the importance of conducting a shear test that simulates the field conditions as accurately as possible. Therefore, in this study, a direct box shear test was conducted within a low normal stress range to determine the shear strength of the interface between the widened embankment soil and a GCL under submerged conditions. No full-scale field tests have been carried out to clarify the behaviour of the embankment laid with a submerged GCL during the construction process. In fact, to our knowledge, the characteristics of the shear strength and the stability of embankments built over GCLs have yet to be adequately studied.

The purpose of this study is to determine the stability of embankments on GCLs, with the intention of providing a safe, stable, and economic method for repairing irrigation ponds using GCLs. A series of shear tests of GCLs were conducted as a novel approach for studying these materials. In summary, this study aims to elucidate the characteristics of the internal shear strength of GCLs without a needle-punched structure as well as the characteristics of the interface between a GCL and the embankment soil. An improved direct box shear test was employed to determine the shear strength of the interface between the soil and GCL using decomposed granite soil and bentonite collected from a GCL as samples. The bentonite was subjected to a consolidated constant pressure direct box shear test under different submersion conditions. Both field tests and direct box shear tests were carried out to clarify the shear strength of bentonite and the shear strength of the interface between bentonite or embankment soil and the geotextiles. Finally, the stability of embankments that incorporated a GCL was evaluated. It should be noted that a study of the issues related to seepage in an embankment and its effects on the water barrier due to the presence of bentonite are beyond the scope of this paper.

Table 1
Physical properties of the soil.

Soil name	Bentonite	Decomposed granite soil (under 0.85 mm)
Natural water content (%)	13.4	1.2
Soil particle density ρ_s (g/cm^3)	2.746	2.655
Liquid limit w_L (%)	501	–
Plastic limit w_p (%)	44	–
Particle size over 2 mm (%)	5.0	–
Particle size under 0.075 mm, over 2 mm (%)	80.0	85.8
Particle size under 0.075 mm (%)	15.0	14.2
Initial water content in GCL (%)	15.0	–
Initial dry density in GCL ρ_d (g/cm^3)	1.248	–

2. Materials and methods

2.1. Test cases and samples

Consolidated constant pressure direct box shear tests were conducted to examine the characteristics of the shear strength for the following cases: (a) granular bentonite, (b) the interface between granular bentonite and geotextiles, (c) decomposed granite soil, and (d) the interface between decomposed granite soil and geotextiles. A GCL in an actual embankment could be integrally sheared on both interfaces between the GCL and soils because the GCL components are bound with a needle-punch. In the laboratory tests conducted in this study, it was assumed that the sliding occurred separately in the interface of each layer in the aforementioned cases. The potential slip surface in the embankment containing a GCL could be estimated by examining these test cases.

A sample of decomposed granite soil (Masado) collected in Yamaguchi city was used in this study. In addition, a sample of a GCL consisting of bentonite sandwiched between woven and non-woven needle-punched geotextiles was analyzed. The physical properties of the samples are listed in Table 1. Fig. 2 shows the grading curves of the decomposed granite soil and granular bentonite. The particle size of bentonite was measured via sedimentation analysis. Bentonite specimens were subjected to the same conditions as a GCL from actual irrigation pond embankments to replicate the swelling of bentonite in the GCL when the GCL is pressed under the widening embankment. Prior to submerging, the initial water content of the bentonite specimens was 15.0% and their dry density was 1.248 g/cm^3. The specimens were submerged and allowed to swell in a direct box shear apparatus under an initial pressure $\sigma_{c0} = 10$ kPa. As illustrated in Fig. 3, the geotextiles were attached to a steel plate during the shear test for the interface between the soil and geotextiles.

2.2. Direct box shear test apparatus

As slope failures can occur along discontinuous planes, Yamamoto et al. (2001) developed a method for evaluating the shear strength along discontinuous planes which can result in slope failures, using a direct shear box test apparatus. In this study, we improved the method used by Yamamoto et al. (2001) to determine the shear strength of the interface between the soil and a GCL. The direct box shear apparatus used in this study is shown in Photo 1. The shear box is composed of an upper and a lower box, and specimens are 6 cm in diameter and 2 cm in height, or 1 cm in height in the case of geotextiles. Silicone grease is applied to reduce the friction on the inside of the shear box. The spacing between the upper shear box and the geotextile is set at 0.2 mm prior to the shearing test. In contrast to ASTM 6243, screws were used to fix the

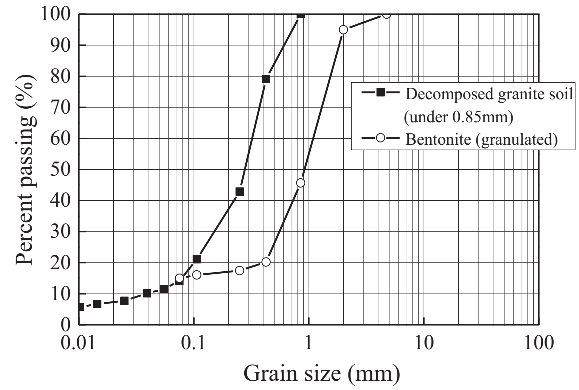

Fig. 2. Grading curves of soil samples used in this study.

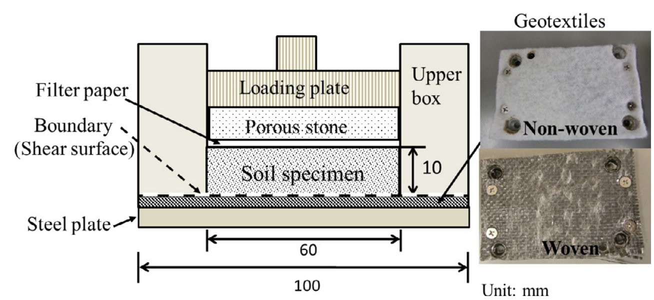

Fig. 3. Cross-section of soil specimens in contact with geotextiles in the shear box.

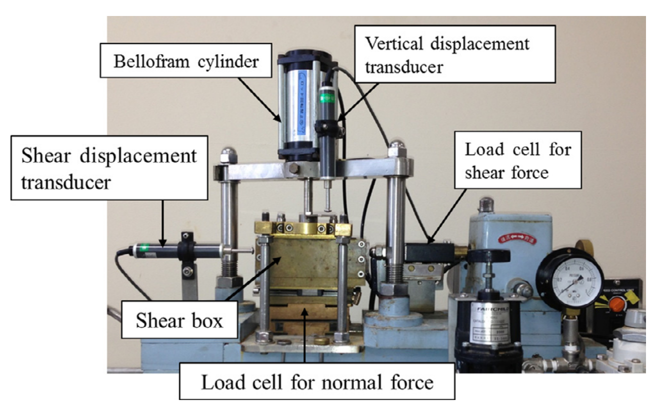

Photo 1. Direct box shear apparatus.

geotextiles. However, since the geotextile was smaller than that recommended in ASTM 6243, the interface between the soil specimen and the geotextile was maintained such that it did not deviate during the shearing. Fox and Stark (2015) suggested that the result of a shear test conducted on a needle-punched reinforced GCL was affected by the specimen size. However, the laboratory tests in this study indicated that the shearing interface between the geotextiles and bentonite or the decomposed granite soil did not include the needle-punched structure. Hence, it can be concluded that the size of the specimen does not influence the results of the shear tests.

2.3. Test procedure for decomposed granite soil and decomposed granite soil with geotextiles

The decomposed granite soil was passed through a 0.85 mm sieve. The sample of decomposed granite soil was first compacted at an optimum moisture content ($w_{opt} = 13.0\%$) determined by a compaction test. Specimens with a diameter of 6 cm and a height of 2 cm were cut from this compacted sample for the direct box shear test.

The shear test of the decomposed granite soil in contact with the geotextiles involved compacting the decomposed granite soil inside the shear box. The specimens were 1 cm in height and had a 90% degree of compaction.

Three specimen types, namely decomposed granite soil, decomposed granite soil with woven geotextiles, and decomposed granite soil with non-woven geotextiles, were consolidated for 30 min under six different pressure values ($\sigma_c = 10$, 20, 30, 50, 75, and 100 kPa). Following consolidation, shearing was conducted under drained conditions, with a shear displacement rate of $v = 0.2$ mm/min as defined by the JGS0561-2000 standards of consolidated constant pressure direct box shear test. Our results confirmed that the shear displacement was not problematic in case of highly permeable soils such as decomposed granite soil.

2.4. Test procedure for bentonite and bentonite with geotextiles

The water content of the bentonite used for the test was adjusted to match that of the bentonite in GCLs, reaching 15.0% (Table 1). All bentonite specimens were compacted within the shear box. The dry density of the specimens was 1.248 g/cm^3, corresponding to that of the bentonite in a GCL. The specimens of bentonite with geotextiles were 1 cm in height.

(a) Unsubmerged conditions

The specimens were consolidated under three different pressures ($\sigma_c = 50$, 75, and 100 kPa). The consolidation was conducted for 30 min for all the specimens. The end of the consolidation time was based on the $3t$ method. Shearing was carried out under unsubmerged conditions with a drainage and a shear displacement rate of $v = 0.02$ mm/min.

(b) One-day and seven-day submersion conditions

Three specimen types, namely bentonite, bentonite with woven geotextiles, and bentonite with non-woven geotextiles, were consolidated under an initial pressure of $\sigma_{c0} = 10$ kPa for 30 min and then submerged for either one day or seven days. Following this process, the specimens submergd for one day were re-consolidated under three different pressures ($\sigma_c = 50$, 75, and 100 kPa) for 24 h. The specimens submergd for seven days were consolidated under five different pressures ($\sigma_c = 20$, 30, 50, 75, and 100 kPa) for 24 h. Shearing was carried out with drainage and a shear velocity of $v = 0.02$ mm/min after 24 h. The shear test was also carried out at $\sigma_{c0} = 10$ kPa. Table 2 presents the initial state of the specimens, the test cases, and the results of the direct box shear tests. In the field test reported in Section 4, the wet unit weight of the decomposed granite soil was $\gamma_t = 19$ kN/m^3. The unit weight was calculated from the water content of the embankments after field shearing and the dry density of 1.600 g/cm^3, which was the compaction condition of the embankments. The thickness of the widening embankments was approximately 0.6 m, and the range of the angle of inclination was $\beta = 34$–46° in the field-loading test. Hence, the normal stress value of the GCL that was pressed by a widening embankment was approximately 10 kPa. It was difficult to conduct a direct box shear test at such low normal stress levels. Therefore, a normal stress range that included the lowest normal stress of 10 kPa was employed in this study.

3. Determination of interface shear strength using direct box shear test

3.1. Strength properties of decomposed granite soil and decomposed granite soil with geotextiles

Fig. 4 shows the shear behaviour of the decomposed granite soil as well as that of the decomposed granite soil in contact with woven or non-woven geotextiles under consolidation pressures of 10 kPa and 100 kPa. The horizontal axis of Fig. 4 represents the shear displacement δ, and the vertical axis represents the shear stress τ and the vertical displacement ΔH. The τ–δ curves for the specimens of decomposed granite soil with geotextiles are slightly lower than those for the specimens of decomposed granite soil when $\sigma_c = 100$ kPa. However, no significant difference was found between the shear behaviours of both sample types with a consolidation pressure of 10 kPa. Thus, there was no difference in their shear behaviours at low normal stress.

As the specimens were compacted at the optimum water content, they generally exhibit an initial contraction that changed to dilation. Dilative behaviour is observed in the

Table 2
Test cases and results from the direct box shearing.

Specimens	Tes No.	Initial water content w_0 (%)	Initial dry density ρ_{d0} (g/cm^3)	Initial consolidation stress σ_{c0} (kPa)	Submersion time (min)	Swelling displacement ΔH_s (mm)	Consolidation stress σ_c (kPa)	Shear strength τ_f (kPa)	Normal stress at failure σ_f (kPa)	Final water content w_f (%)
Decomposed granite soil	DGA-1	13.5	1.642	–	1440	–	10	37.0	27.1	38.1
	DGA-2	13.2	1.631	–	1440	–	20	48.4	38.4	32.2
	DGA-3	13.1	1.633	–	1440	–	30	88.5	85.0	29.4
	DGA-4	13.5	1.650	–	1440	–	50	107.6	89.2	21.5
	DGA-5	13.4	1.634	–	1440	–	75	154.0	140.1	24.5
	DGA-6	12.9	1.630	–	1440	–	100	171.7	154.6	23.7
Decomposed granite soil + geotextiles (non-woven)	DGN-1	13.4	1.630	–	1440	–	10	41.2	36.2	31.5
	DGN-2	13.2	1.641	–	1440	–	20	55.7	52.3	30.9
	DGN-3	12.8	1.642	–	1440	–	30	59.5	52.6	29.7
	DGN-4	12.9	1.628	–	1440	–	50	94.5	91.0	21.7
	DGN-5	12.9	1.632	–	1440	–	75	128.9	134.9	24.5
	DGN-6	13.3	1.636	–	1440	–	100	169.2	190.3	21.4
Decomposed granite soil + geotextiles (woven)	DGW-1	13.5	1.636	–	1440	–	10	41.6	23.9	34.2
	DGW-2	12.9	1.657	–	1440	–	20	45.6	39.4	29.3
	DGW-3	12.5	1.646	–	1440	–	30	48.8	42.0	31.3
	DGW-4	13.3	1.622	–	1440	–	50	106.6	110.0	24.0
	DGW-5	13.1	1.630	–	1440	–	75	123.1	141.3	24.5
	DGW-6	13.1	1.622	–	1440	–	100	133.7	159.3	23.7
Bentonite	BAU-1	13.8	1.203	–	–	–	50	138.6	103.9	13.7
	BAU-2	13.2	1.258	–	–	–	75	196.7	156.8	12.8
	BAU-3	13.9	1.251	–	–	–	100	261.2	201.1	15.0
	BA-1	14.8	1.252	10	1440	4.78	50	58.0	53.0	71.3
	BA-2	14.9	1.222	10	1440	4.25	75	70.1	69.0	38.8
	BA-3	19.1	1.227	10	1440	4.55	100	91.1	96.9	60.3
	BA-7.1	14.9	1.252	10	10,080	8.21	10	24.3	21.0	78.7
	BA-7.2	15.1	1.250	10	10,080	8.23	20	23.2	29.3	84.2
	BA-7.3	14.7	1.252	10	10,080	8.42	30	27.9	35.1	70.7
	BA-7.4	15.0	1.248	10	10,080	8.09	50	27.6	48.6	77.8
	BA-7.5	15.3	1.235	10	10,080	8.10	75	31.4	82.2	78.8
	BA-7.6	14.6	1.247	10	10,080	7.86	100	50.2	111.0	68.0
Bentonite + geotextiles (non-woven)	BN-1	15.1	1.247	10	1440	2.67	50	41.0	66.4	33.9
	BN-2	13.9	1.229	10	1440	3.22	75	44.8	81.9	51.0
	BN-3	16.3	1.223	10	1440	3.09	100	65.1	133.6	46.8
	BN-7.1	15.2	1.249	10	10,080	5.98	10	13.3	21.1	103.5
	BN-7.2	15.2	1.249	10	10,080	5.95	20	20.6	20.6	84.3
	BN-7.3	15.5	1.255	10	10,080	5.98	30	27.6	32.1	84.5
	BN-7.4	14.9	1.246	10	10,080	5.97	50	41.2	79.8	80.5
	BN-7.5	15.2	1.249	10	10,080	5.77	75	49.8	116.0	85.1
	BN-7.6	15.3	1.248	10	10,080	5.89	100	61.1	131.0	69.7

(*continued on next page*)

Table 2 (*continued*)

Specimens	Tes No.	Initial water content w_0 (%)	Initial dry density ρ_{d0} (g/cm^3)	Initial consolidation stress σ_{c0} (kPa)	Submersion time (min)	Swelling displacement ΔH_s (mm)	Consolidation stress σ_c (kPa)	Shear strength τ_f (kPa)	Normal stress at failure σ_f (kPa)	Final water content w_f (%)
Bentonite	BW-1	15.1	1.279	10	1440	2.67	50	42.3	57.1	26.6
+ geotextiles	BW-2	13.9	1.249	10	1440	2.55	75	51.4	80.8	30.0
(woven)	BW-3	15.2	1.221	10	1440	3.21	100	63.9	106.1	23.0
	BW-7.1	15.4	1.247	10	10,080	5.27	10	15.9	23.8	93.9
	BW-7.2	14.6	1.253	10	10,080	5.25	20	18.2	20.7	93.4
	BW-7.3	15.5	1.252	10	10,080	5.08	30	18.4	29.0	84.2
	BW-7.4	14.8	1.247	10	10,080	5.16	50	27.9	52.3	72.6
	BW-7.5	14.5	1.247	10	10,080	5.09	75	37.7	83.9	71.0
	BW-7.6	14.7	1.242	10	10,080	5.17	100	48.4	103.2	69.7

case of decomposed granite soil with non-woven geotextiles under $\sigma_c = 10$ kPa. In contrast, the specimens of decomposed granite soil with woven geotextiles exhibit contractive behaviour during shearing under the same conditions. The dilative behaviour of decomposed granite soil with non-woven geotextiles under a consolidation pressure of 10 kPa could be caused by the formation of linkages between the decomposed granite soil and non-woven geotextiles. As the non-woven geotextile material is similar to cloth, adhesion may be caused by the entanglement of fibres resulting in dilation during shearing.

Fig. 5 shows three failure lines, one each for the decomposed granite soil, decomposed granite soil with woven geotextiles, and decomposed granite soil with non-woven geotextiles. In contrast to the results for the decomposed granite soil, the interface between the decomposed granite soil and both types of geotextiles show a lower internal friction angle, denoted by ϕ_d and a higher cohesion, denoted by c_d.

Whether the geotextiles are woven or non-woven had no impact of the difference in the value of ϕ_d. However, it can be observed that the value of c_d for the specimens of decomposed granite soil with non-woven geotextiles is slightly lower than that of the specimens of decomposed granite soil with woven geotextiles. Hence, the difference in the shear strength is based on whether the geotextile material is woven or non-woven. Voids in the fibres of the non-woven geotextiles are larger than those in the woven geotextiles, thereby increasing the possibility that soil particles could enter.

3.2. Swelling and strength properties of bentonite and bentonite with geotextiles

Fig. 6 shows the typical swelling behaviour of bentonite and bentonite with woven and non-woven geotextiles following seven days of submersion under $\sigma_{c0} = 10$ kPa (Test numbers: BA-7.1, BN-7.1, BW-7.1). In this figure, the swelling displacement showed positive values. The specimen exhibits uniform swelling of approximately 5–8 mm under $\sigma_{c0} = 10$ kPa. A maximum swelling displacement of 8.3 mm is observed in a bentonite sample submerged for 14 days prior to the measurement. As shown in Fig. 6, no significant difference was found in the swelling displacement for the submersion periods of seven days and 14 days. Therefore, it can be concluded that the amount of swelling reached a steady state after seven days of submersion.

In contrast, following a seven-day submersion period, the swelling displacement of the bentonite with geotextile specimen is less than that of the bentonite specimens. This may be caused by the reduced height of bentonite in the samples. The difference in the swelling displacement is also affected by the presence of woven or non-woven geotextiles. The two different geotextile materials showed a difference in the drainage between bentonite and the geotextiles.

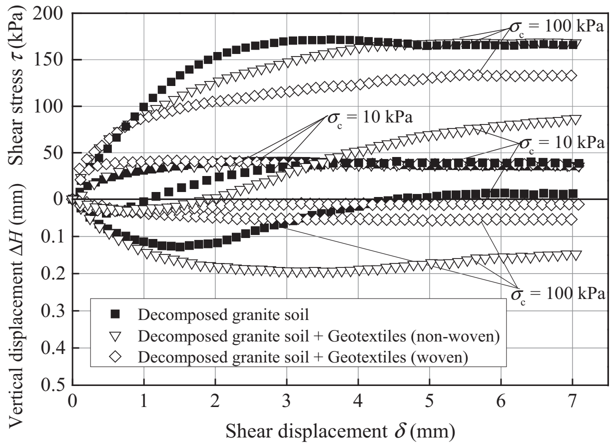

Fig. 4. Shear behaviour of the decomposed granite soil as well as decomposed granite soil with woven and non-woven geotextiles with $\sigma_c = 10$ and 100 kPa.

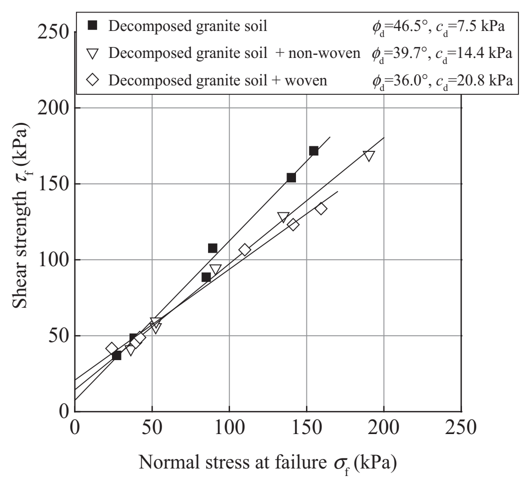

Fig. 5. Failure lines of the decomposed granite soil as well as decomposed granite soil with woven and non-woven geotextiles.

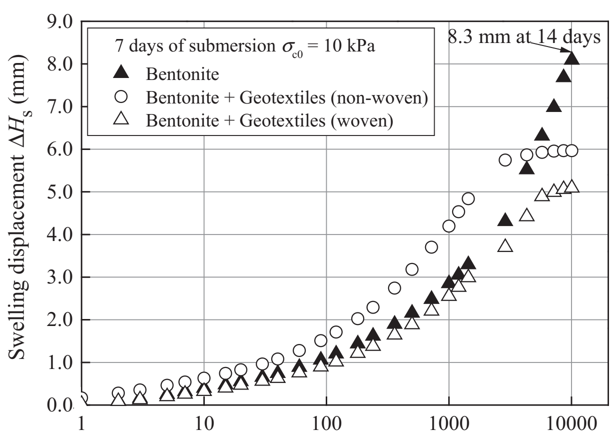

Fig. 6. Swelling behaviour of the bentonite as well as bentonite with woven and non-woven geotextiles for a submersion period of seven days.

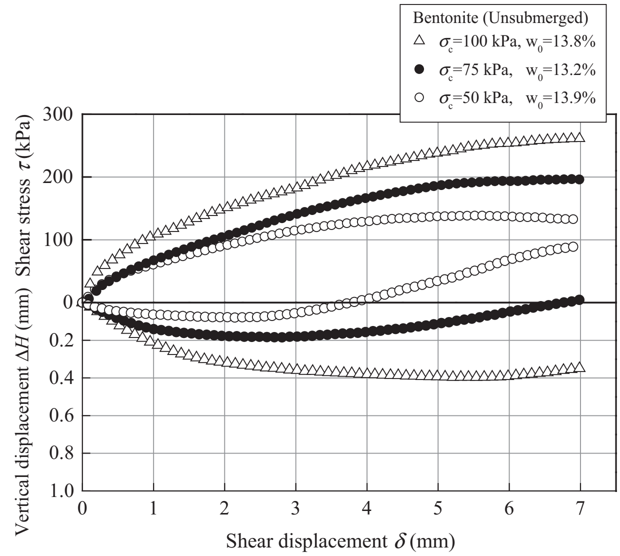

Fig. 7. Shear behaviour of the unsubmerged bentonite.

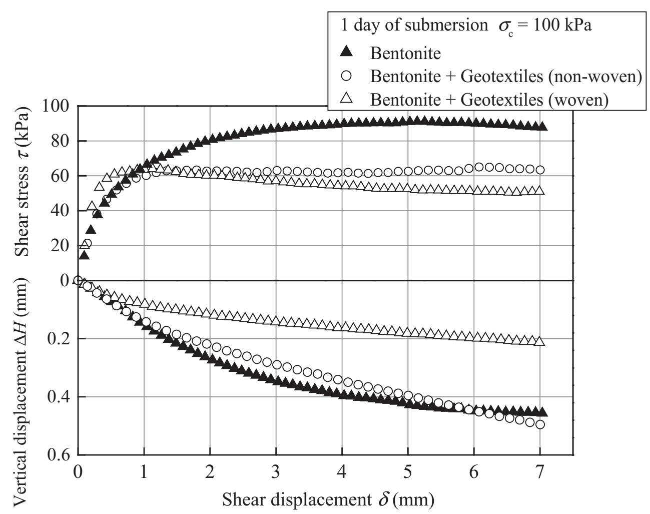

Fig. 8. Shear behaviour of the bentonite as well as that of bentonite with woven and non-woven geotextiles with $\sigma_c = 100$ kPa for a submersion period of one day.

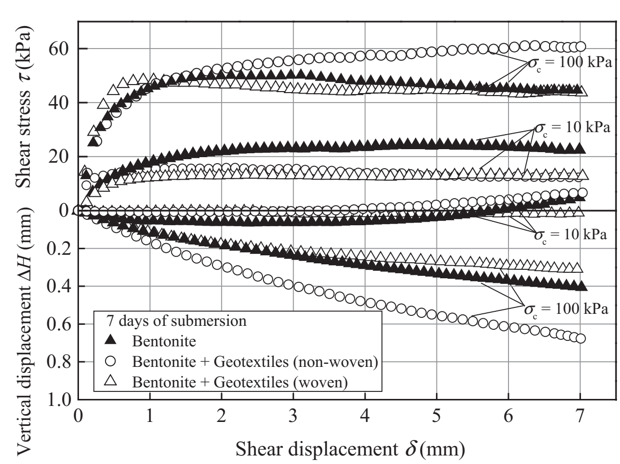

Fig. 9. Shear behaviour of the bentonite as well as that of bentonite with woven and non-woven geotextiles with $\sigma_c = 10$ and 100 kPa for a submersion period of seven days.

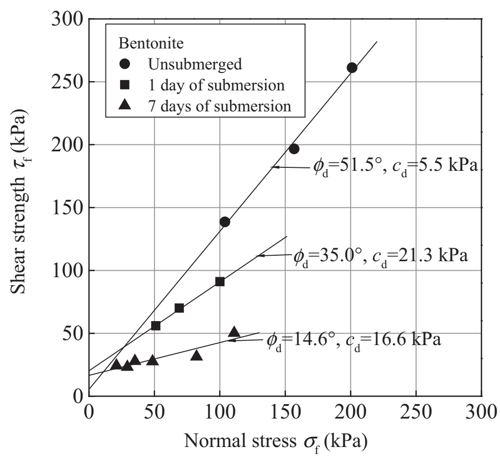

Fig. 10. Failure lines of the bentonite under different submersion conditions.

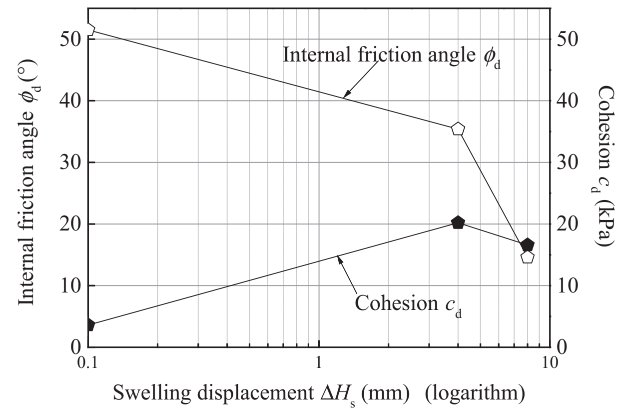

Fig. 11. Change in strength parameters with respect to swelling displacement.

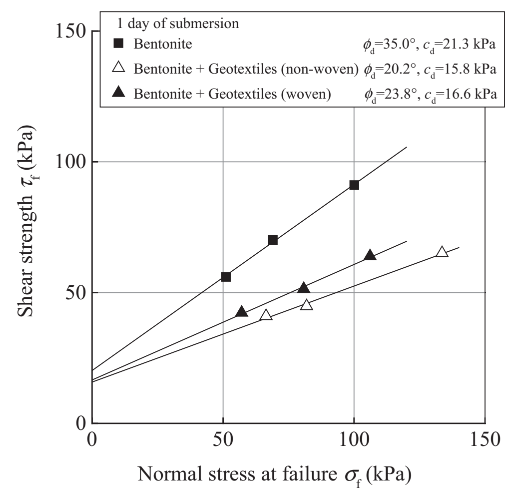

Fig. 12. Failure lines of bentonite as well as bentonite with woven and non-woven geotextiles for a submersion period of one day.

Fig. 7 illustrates the shear behaviour of unsubmerged bentonite under different consolidation pressures. Fig. 8 depicts the shear behaviour of bentonite and bentonite with woven and non-woven geotextiles after a one-day submersion period under a consolidation pressure of 100 kPa. In the case of the unsubmerged samples, the value of τ monotonically increases with increased shearing. In contrast, after a submersion period of one day, the value of τ is observed to increase monotonically during the early stages of shearing before becoming almost constant in all the samples of bentonite. In Fig. 8, the τ–δ curves of the specimens of bentonite with geotextiles are lower than those of the specimens of bentonite, and τ shows a steady state after $\delta = 3$ mm.

The shear behaviours of bentonite and bentonite with woven and non-woven geotextiles following seven days of submersion under consolidation pressures of 10 kPa and 100 kPa are shown in Fig. 9. The τ–δ curves are low when compared with those of the one-day submersion. The value of τ monotonically increases during the early stages of shearing before becoming steady. This is similar to bentonite under seven days of submersion. With respect to ΔH, the specimens of bentonite with woven geotextiles always contract under pressures of 10 kPa, while bentonite with non-woven geotextiles dilated. In summary, we found that the adhesion formed between bentonite and non-woven geotextiles is higher than that between decomposed granite soil and woven geotextiles.

Fig. 10 shows the failure lines for bentonite under different submersion conditions. The normal stress in the figure corresponds to the total stress on the horizontal upper surface of the specimen during shearing. Volumetric changes of the bentonite specimens are measured during shearing. Therefore, it can be concluded that the bentonite specimens are sheared under the drained condition. Additionally, the bentonite specimens experienced a pressure of $\sigma_{c0} = 10$ kPa during hydration and were thus not under swelling-free conditions. The value of ϕ_d for the unsubmerged bentonite is very high. This tendency is consistent with that observed in the consolidation process. This may be caused by the solidity of the granulated bentonite prior to the absorption of water. Moreover, the c_d of the unsubmerged bentonite is 5.5 kPa. Generally, the cohesion of normally consolidated clay is zero when the specimen is formed from the slurry state. However, in this study, the bentonite specimens are composed of granulated bentonite and formed by the compaction method. As a result, slight cohesion is observed.

The strength parameters of bentonite submerged for seven days are lower than those of decomposed granite soil and of bentonite submerged for one day. The bentonite particles in all specimens softened and swelled due to the absorption of water during the seven-day submersion. It is suspected that the internal friction angle decreases, and the shear plane becomes smoother under these conditions. Fig. 11 shows the relationship between the swelling displacements of bentonite and their strength parameters. The internal friction angle of bentonite decreases with increased swelling displacement by submersion. However, cohesion increases after one day of submersion but

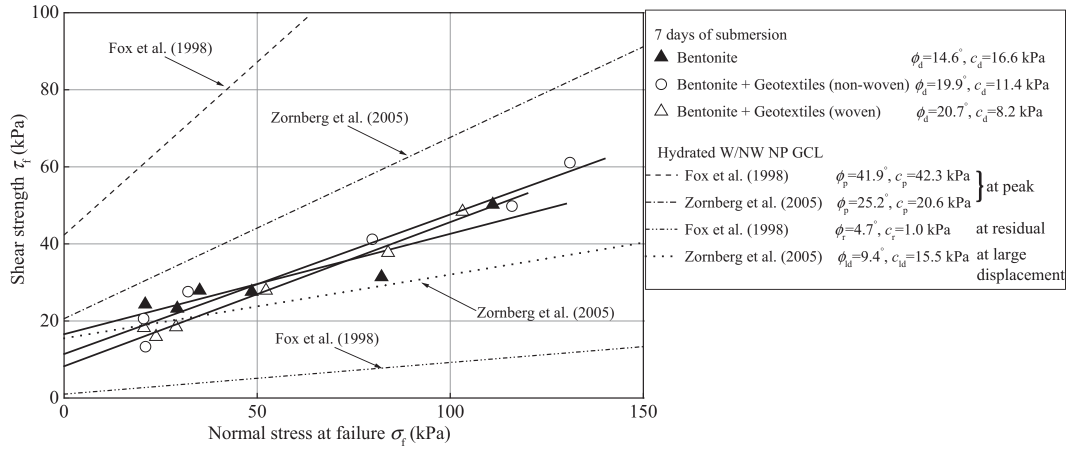

Fig. 13. Failure lines of the bentonite as well as bentonite with woven and non-woven geotextiles for a submersion period of seven days.

decreases after seven days. Fig. 12 shows the failure lines of bentonite with geotextiles that were submerged for one day. In this case, the interfacial strength between bentonite and geotextiles is lower than those in bentonite. No significant differences were found between the values for the two types of geotextiles. Fig. 13 displays the failure lines of bentonite with geotextiles submerged for seven days. The values of ϕ_d in this case are similar to those of bentonite with geotextiles submerged for one day, as shown in Fig. 12. However, the values of c_d are lower than that of bentonite with geotextiles submerged for one day. As illustrated in Fig. 13, the value of ϕ_d for bentonite submerged for seven days is lower. Nevertheless, the value of c_d is higher than that for bentonite with geotextiles as the specimens are sheared at the interface between bentonite and the geotextiles. Fig. 13 shows the failure lines that were observed under previous shear tests conducted on hydrated GCLs in which woven and non-woven geotextiles were sandwiched and reinforced by a needle-punched structure (Fox et al., 1998a; Zornberg et al., 2005). The values of c_p and ϕ_p, c_r and ϕ_r, and c_{ld} and ϕ_{ld} were determined based on peak (p), residual (r), and large displacement (ld) shear strengths, respectively. Zornberg et al. (2005) used a direct shear apparatus with a maximum shear displacement of 75 mm, whereas the apparatus used by Fox et al. (1998a) had a maximum shear displacement of 203 mm. Fox and Stark (2015) suggested that residual shear strengths of most GCLs and GCL interfaces could not be measured using a shear apparatus with maximum shear displacement in the range of 50–100 mm. However, a shear apparatus with a maximum shear displacement of 203 mm could measure the residual shear conditions of GCLs.

Fig. 13 compares the failure lines observed in the current study with those observed in previous studies. It is found that the values of c_d and ϕ_d for each bentonite and bentonite with geotextiles specimen in our work are lower than c_p and ϕ_p obtained in the previous studies. This is due to the presence or absence of needle-punches inside the specimens. Furthermore, the values of ϕ_d in our work are found to be higher than ϕ_{ld}. The values of c_d for the interface between bentonite and both geotextiles are lower than c_{ld}, whereas the value of c_d for bentonite is close to c_{ld}. These results suggest that the shear force resistance of the

Photo 2. Panoramic view of dam embankments under construction.

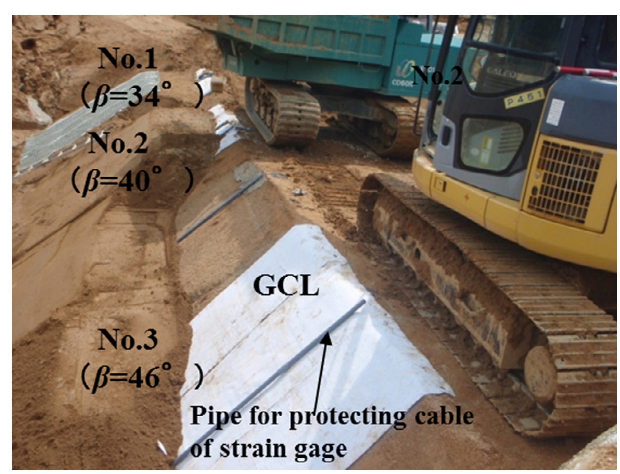

Photo 3. Embankments with different slope angles.

needle-punches is present in case of large displacement shear strengths. As shown in Fig. 13, ϕ_r and c_r have the lowest strength parameters. The value of ϕ_d for bentonite is consistent with that obtained by Kamai and Miyata (1993), who reported the results of direct box shear tests on bentonite.

4. Field failure test on real embankment for irrigation pond

Three embankment bodies were constructed from the decomposed granite soil with inclination angles $\beta = 34°$, 40° and 46°, on a site in Yamaguchi City. After six months of submergence, field-loading tests were conducted, and measurements were performed for determining the water content of bentonite in the GCL placed inside the embankment body and floating in the pond. A panoramic view of the embankments at the test site is shown in Photo 2. The embankments are vertically compacted to the foundation ground. The construction of the embankments is depicted in Photo 3. Fox et al. (1998b) established that damages to GCLs were minor when the depth of the soil cover was 305 mm or more. In this study, widened embankments with thicknesses of approximately 0.6 m were used. Additionally, it was observed that the normal stress on the GCL increased with an increase in the thickness of the widening embankment. No damage to the GCLs was observed during the construction of the embankments (Photo 3). Strain gauges, for measuring the displacement around the GCLs, were embedded in each embankment (Photo 3). The soil samples comprising the in-situ decomposed granite soil and the woven and non-woven needle-punched GCLs were the same as those used in the laboratory tests. After six months, the reservoir water was removed using a pump to conduct field-loading tests. During construction and submersion, no deformation such as sliding or settlement caused by changes in the water content of bentonite in the GCLs in the embankments was observed. Additionally, the water level was situated at the top of the widened slope (Photo 4). Moreover, the adjacent surface of each embankment was cut off prior to shearing. As shown in Photo 5, a vertical load was applied to the top surface of the widened embankments with a backhoe. During the field-loading test, the vertical load and the bending strain were continuously measured by a load cell underneath a bucket of the backhoe and the strain gauges embedded by GCLs, respectively. The field-loading test was conducted with step-loading, and it took approximately 30 min to complete the test. The maximum value of the bending strain generated during the loading was very small in each test case. Thus, the shear strain was also estimated to be small, and therefore, the strain rate was considered to be slow. It was possible to conduct the field-loading test under drained conditions. However, no slippage was observed in the embankments even under these conditions. Therefore, the top part of the slope of the widened embankment was removed, and the loading test was conducted again as illustrated in Fig. 14. Fig. 15 displays the relationship between the bending strain and the applied load, T, in the three different embankments. It should be noted that the maximum load T_{max} was not preset. Bending strains were measured only during shearing, and therefore, it was not clear whether any bending strains

Photo 5. Loading test on the upper surface of embankment.

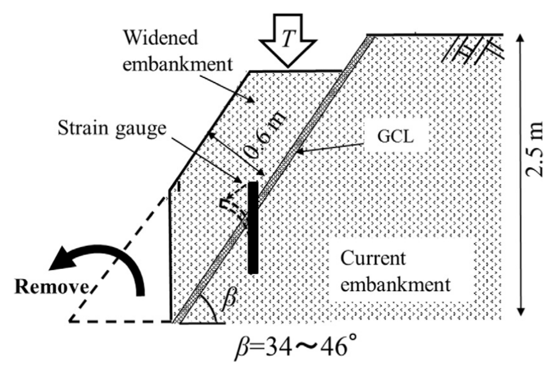

Fig. 14. Configuration of the widened embankments for field loading test.

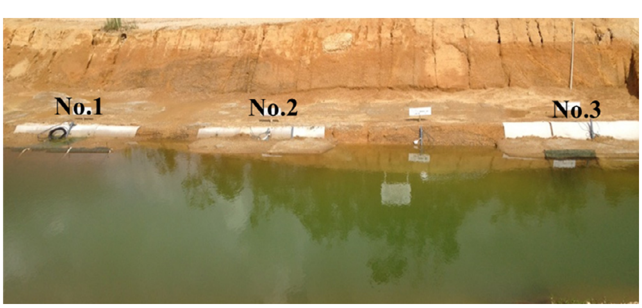

Photo 4. Submersion of embankments.

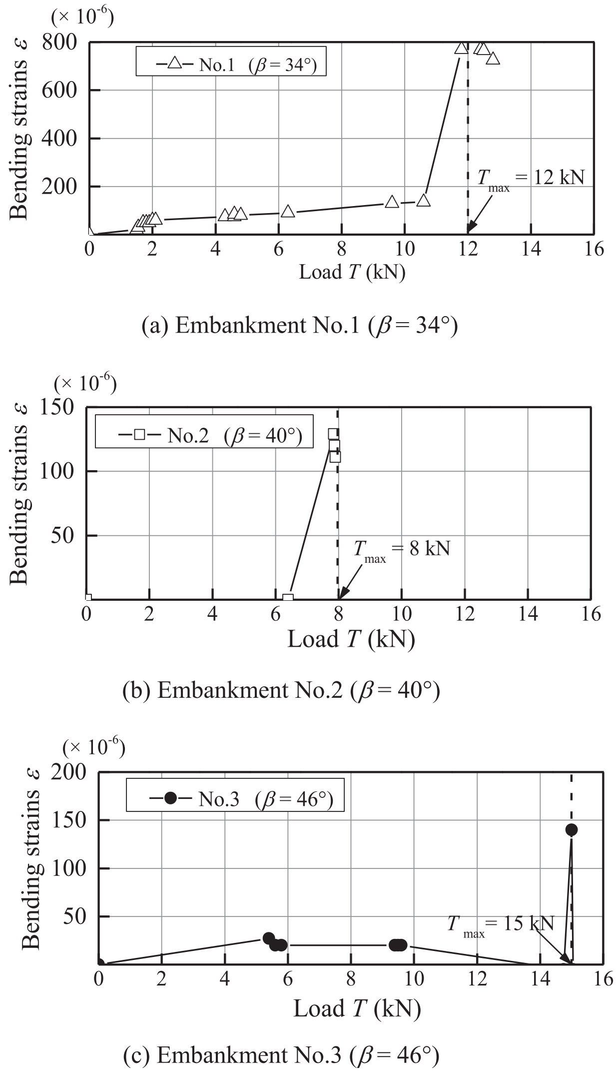

(a) Embankment No.1 ($\beta = 34°$)

(b) Embankment No.2 ($\beta = 40°$)

(c) Embankment No.3 ($\beta = 46°$)

Fig. 15. Variation of the bending strains with loading.

Table 3
Comparison of water content in embankment body and GCLs.

No.	Angle of inclination β (°)	Water content of bentonite in GCL (%)	Water content of granitic soil backfill (%)
1	34	151.9	20.1
2	40	145.7	19.8
3	46	180.4	24.3

occurred when the embankments were submerged. The maximum load was measured during the shearing of each embankment. In each embankment, minute strains occurred under an applied load, and no sliding failure as such was observed. As a result, shearing failure was not observed even for embankments with a maximum slope angle of 46°. It seems that the yield criterion of the slope of the widened embankment was not fulfilled when shear stress was applied by the surcharge load. A shear plane was not prescribed in the field-loading test. In addition, the widened part on which the vertical loading was imposed was placed on the original embankment via a GCL. It has a complex structure composed of different parts. Therefore, the stresses normal and tangential to the shear plane were not uniform because of the field loading. However, as indicated by the direct box shear tests in the present study, the GCL did not necessarily represent a weak point in an embankment.

Table 3 presents the water content of the embankment bodies and GCLs that were submerged for six months. The water content of the soil was measured immediately after completion of the shear tests. The natural water content of bentonite in GCL is 15.0%. However, after six months, the natural water content is observed to increase by approximately 150–180%. The confining stress decreases with increase in the inclination angle of the slope. Therefore, the GCL water content is different in the three embankments. In comparison, the natural water content of the granitic soil backfills is 13.0%, which increased by 20–24% after six months. The in-situ water content of bentonite in a GCL embedded in an actual embankment is approximately 150%. Conversely, the final water content of bentonite in the laboratory test is in the range of 60–100% (Table 2). The water content of bentonite in the laboratory test is lower than that in the field test. This could be because of the following reasons. First, the swelling of bentonite specimens in the shear box was restricted to a single dimension. Second, the GCL in the actual embankment may be subjected to any arbitrary shear stress, during the swelling, owing to the slope, whereas no shear stress was imposed on the specimen in the laboratory test during swelling.

Furthermore, the water content of bentonite in a GCL floating in the pond was periodically measured. As shown in Fig. 16, the water content increases during the submersion for ten days but became almost constant after this time period. This reveals that the widened embankment acted to restrain the swelling of bentonite in the GCL. Although the liquid limit of the bentonite used in this study was approximately 500%, the water content of bentonite in the GCL, even without a widening embankment, is approximately 300%. This suggests that the needle-punched structure in a GCL also restrained the swelling of bentonite. This is consistent with the findings of Lake and Rowe (2000) and Fox et al. (2000), who reported the effects of needle punching on bentonite swelling.

The conditions in the laboratory and field tests are summarized as follows: (1) The normal stress set in the laboratory covered the lowest normal stress of 10 kPa, which is equivalent to the in-situ normal stress; (2) The swelling time and water content after swelling were different for the laboratory and field test and the difference in the water content of bentonite for field and laboratory tests may well be attributed to how the soils were geometrically constrained during swelling in the tests; (3) Because the

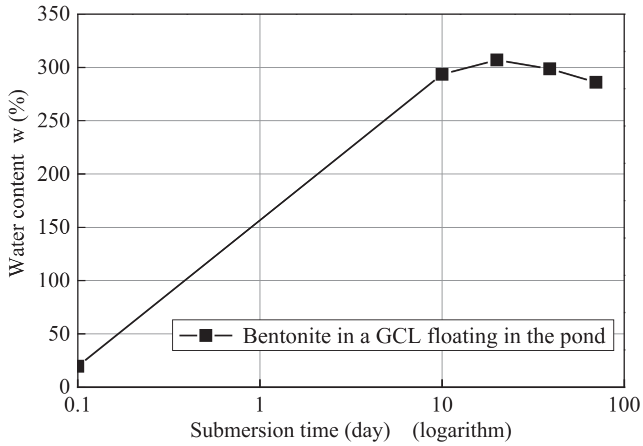

Fig. 16. Changes in water content of the bentonite in a GCL floating in the pond with submersion time.

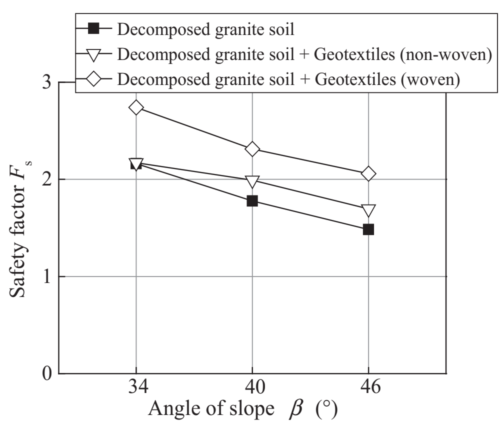

Fig. 17. Changes in the safety factor of widened embankment made from decomposed granite soil or decomposed granite soil with woven or non-woven geotextiles with the angle of slope.

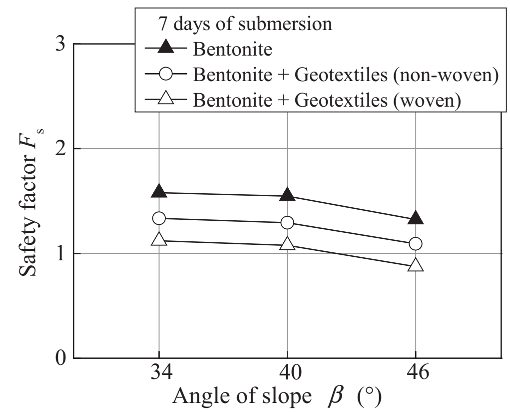

Fig. 18. Changes in the safety factor of widened embankment made from bentonite or bentonite with woven or non-woven geotextiles with the angle of slope.

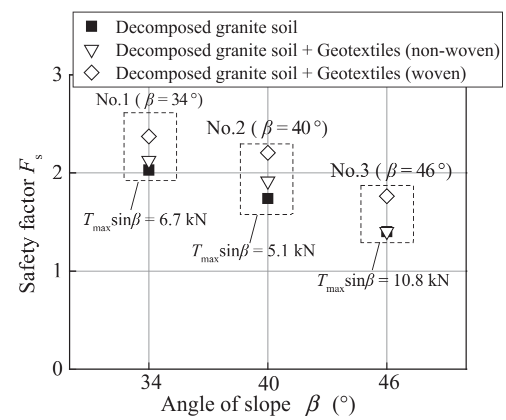

Fig. 19. Comparison of the safety factors of widened embankment made from decomposed granite soil or decomposed granite soil with woven or non-woven geotextiles under different loading conditions.

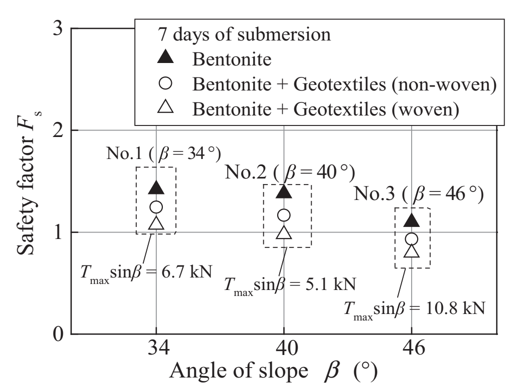

Fig. 20. Comparison of the safety factors of widened embankment made from bentonite or bentonite with woven or non-woven geotextiles under different loading conditions.

laboratory and field tests were carried out under a drained condition, the field conditions were accurately simulated by the laboratory tests.

5. Stability analysis for embankment using GCL

The stability of an embankment using a GCL is discussed in this section. As illustrated in Fig. 14, the safety factors related to sliding failure were calculated for six conditions: decomposed granite soil, the interface between decomposed granite soil and woven and non-woven geotextiles, bentonite, and the interface between bentonite and woven and non-woven geotextiles. The safety factor calculations utilized the strength parameters obtained from the direct box shear test. It should be noted that the interfacial shear strength obtained from the laboratory test did not include any effects of the needle-punch. Three widened embankments of different weights—$W = 65.6$, 57.2, and 58.5 kN—were also used. The weights were measured in the field test (Photo 3). The angles of inclination were $\beta = 34°$, 40°, and 46°, and the sliding surface length was $l = 2.7$ m for the three embankments. The pore water pressure and the thickness and weight of the GCL were omitted from the calculation. Thus, the safety factor was deduced from the following equation:

$$F_s = \frac{W \cos\beta \tan\phi_d + c_d l}{W \sin\beta} \tag{1}$$

Figs. 17 and 18 show the safety factors with respect to the sliding failure of decomposed granite soil and bentonite after seven days of submersion. Generally, the value of F_s decreases as β increases. The value of c_d is highest in the interface between decomposed granite soil and woven geotextiles. Therefore, the value of F_s (2.7) is greater than 2.0 in this case. In contrast, the value of F_s in the interface between bentonite and woven geotextiles at $\beta = 46°$ is the lowest, with $F_s = 0.8$. With the exception of this case, the value of F_s is always greater than 1.0.

Additionally, Figs. 19 and 20 show a comparison of safety factors for the sliding failure with respect to an applied loading, T (kN), when the maximum strain was obtained in the field shear test (Fig. 15). In these calculations, the assumptions and strength parameters are the same as those for the previous calculations (Figs. 17 and 18; Eq. (1)). The safety factor was deduced from the following equation (Eq. (2)) in which the three embankments were represented by the value of T, which was obtained from the embankments during loading (Fig. 15).

$$F_s = \frac{\{(T+W)\cos\beta\tan\phi_d\} + c_d l}{(T+W)\sin\beta} \tag{2}$$

The values of F_s for the decomposed granite soil and decomposed granite soil with geotextiles are greater than 1.0 in all the cases. In contrast, the values of F_s for the interface between bentonite and both geotextiles at $\beta = 46°$ were less than 1.0. Despite these values of F_s from the stability analysis (Figs. 18 and 20), sliding failure was not visually observed in the field shear tests. It seems that the needle-punched structure may have prevented the sliding failure at the interface between bentonite and both geotextiles. It is possible that a sliding failure may occur at the interface between a widened embankment and the GCL when excess pore water pressure is generated in the lower surface of a GCL, possibly due to a rapid change in the water level of a pond or a strong vibration of an earthquake. Hence, it is necessary to investigate the seismic performances of GCLs in irrigation pond embankments.

6. Conclusions

In this study, a series of direct box shear tests were conducted to determine the shear strength between bentonite or decomposed granite soil and a GCL. Field-loading tests were also conducted to investigate the failure behaviour of an embankment body laid with GCLs. Finally, the stability of widened embankment bodies containing GCLs was calculated and evaluated. The main findings of the present study can be summarized as follows:

(1) The shear strength of the interface between decomposed granite soil and woven or non-woven geotextiles was lower than that of decomposed granite soil. The cohesion, in particular, differed depending on whether the geotextiles were woven or non-woven.

(2) The shear strength of bentonite decreased with an increase in swelling. After seven days of submersion, the shear strength of bentonite as well as that of the interface between bentonite and the geotextiles was reduced. Furthermore, in the bentonite specimens, ϕ_d was lower and c_d was higher than those in specimens with geotextiles.

(3) Stability of the embankment was evaluated from the results of the direct box shear tests. A maximum safety factor, F_s of 2.7, was calculated for the interface between decomposed granite soil and woven geotextiles, while a minimum F_s of 0.8 was calculated for the interface between bentonite and woven geotextiles. The F_s of the interface between bentonite and geotextiles could have been improved by the presence of a needle-punched structure. Even though the interface between decomposed granite soil and geotextiles was not reinforced by needle punching, the value of F_s was still high.

(4) A field-loading test was conducted for embankments laid with GCL. The load on the widened embankment induced a shearing failure. However, the shear displacement was minuscule and no deformation was observed.

(5) Stability of the embankment was evaluated from the results of the field-loading test as well. As in the case of the shear tests, the F_s values for decomposed granite soil as well as decomposed granite soil with geotextiles were greater than 1.0 in all cases. In contrast, the F_s values were less than 1.0 at the interface between bentonite and both geotextiles at $\beta = 46°$ with $T = 10.8$ kN. However, sliding failure was not observed in the field shear test. It is possible that the needle-punched structure prevented sliding failure at the interface between the bentonite and both geotextiles.

Therefore, it can be concluded that the GCLs, consisting of bentonite sandwiched between woven and non-woven geotextiles, had a small negative influence on the stability of the embankment. Therefore, the use of GCLs to repair dam embankments can be considered safe.

Acknowledgement

The study was financially supported by the Ministry of Agriculture, Forestry and Fisheries. We express our sincere thanks to them.

References

Anubhav, Basudhar, P.K., 2010. Modeling of soil–woven geotextile interface behavior from direct shear test results. Geotext. Geomembr. 28 (4), 403–408.

ASTM D 6243. Standard test method for determining the internal and interface shear resistance of geosynthetic clay liner by the direct shear method.

Athanassopoulos, C., Yuan, Z., 2011. Correlation between needlepunch-reinforced geosynthetic clay liner peel strength and internal shear strength. In: Han, J., Alzamora, D. (Eds.), Geo-Frontiers 2011, ASCE, pp. 1922–1930.

Bacas, B.M., Blanco-Fernandez, E., Cañizal, J., 2013. Comparison of the adhesion and shear tensile strength of needle-punched GCLs. Geotext. Geomembr. 41, 17–25.

Bouazza, A., 2002. Geosynthetic clay liners. Geotext. Geomembr. 20 (1), 3–17.

Chen, Y.-M., Lin, W.-A., Zhan, T.L.T., 2010. Investigation of mechanisms of bentonite extrusion from GCL and related effects on the shear strength of GCL/GM interfaces. Geotext. Geomembr. 28 (1), 63–71.

Daniel, D.E., Koerner, R.M., 2007. Geosynthetic clay liners. In: Daniel, D.E., Koerner, R.M. (Eds.), Waste Containment Facilities, ASCE, New York, pp. 207–226.

Fox, P.J., Rowland, M.G., Scheithe, J.R., 1998a. Internal shear strength of three geosynthetic clay liners. J. Geotech. Geoenviron. Eng., ASCE 124 (10), 933–944.

Fox, P.J., Triplett, E.J., Kim, R.H., Olsta, J.T., 1998b. Field study of installation damage for geosynthetic clay liners. Geosynth. Int. 5 (5), 491–520.

Fox, P.J., De Battista, D.J., Mast, D.G., 2000. Hydraulic performance of geosynthetic clay liners under gravel cover soils. Geotext. Geomembr. 18 (2–4), 179–201.

Fox, P.J., 2010. Internal and interface shear strengths of geosynthetic clay liners. Keynote lecture. In: 3rd International Symposium on GCLs, Würzburg, Germany, pp. 203–218

Fox, P.J., Sura, J.M., Nye, C.J., 2015. Dynamic shear strength of a needle-punched GCL for monotonic loading. J. Geotech. Geoenviron. Eng., ASCE 141 (7), 04015025-1–04015025-8.

Fox, P.J., Stark, T.D., 2015. GCL shear strength and its measurement-ten-year update. Geosynth. Int. 22 (1), 3–47.

Gilbert, R.B., Fernandez, F., Horsfield, D.W., 1996. Shear strength of reinforced geosynthetic clay liner. J. Geotech. Eng. 122 (4), 259–266.

Goodhue, M.J., Edil, T.B., Benson, C.H., 2001. Interaction of foundry sands with geosynthetics. J. Geotech. Geoenviron. Eng., ASCE 127 (4), 353–362.

Hara, T., Sakota, K., Fujita, M., Kochi, Y., 2009. Efficacy of inner bentonite matting for controlling seepage in irrigation tank embankment. J. Irrig., Drain. Rural Eng. 77 (1), 124–125 (in Japanese).

Hurst, P., Rowe, R.K., 2006. Average bonding peel strength of geosynthetic clay liners after short-term exposure to water and jet fuel A-1. Geotext. Geomembr. 24 (1), 58–63.

JGS0561-2000. Method for consolidated constant pressure direct box shear test on soils.

Kamai, T., Miyata, Y., 1993. Failure propagation process in a landslide cohesive soil subjected to direct shear. Landslides 29 (4), 9–17 (in Japanese).

Katsumi, T., Ishimori, H., Onikata, M., Fukagawa, R., 2008. Long-term barrier performance of modified bentonite materials against sodium and calcium permeant solutions. Geotext. Geomembr. 26 (1), 14–30.

Khoury, C.N., Miller, G.A., Hatami, K., 2011. Unsaturated soil-geotextile interface behavior. Geotext. Geomembr. 29 (1), 17–28.

Kodaka, T., Teramoto, Y., 2009. Shear failure properties of compacted bentonite under unsaturated and saturated conditions. Jpn. Geotech. J. 4 (1), 59–69 (in Japanese).

Komine, H., Ogata, N., 1994. Experimental study on swelling characteristics of compacted bentonite. Can. Geotech. J. 31 (4), 478–490.

Lee, K.M., Manjunath, V.R., 2000. Soil–geotextile interface friction by direct shear tests. Can. Geotech. J. 37 (1), 238–252.

Lake, C.B., Rowe, R.K., 2000. Swelling characteristics of needlepunched thermally treated geosynthetic clay liners. Geotext. Geomembr. 18 (2), 77–101.

Lee, J., Shackelford, C., 2005. Concentration dependency of the prehydration effect for a GCL. Soils Found. 45 (4), 27–41.

Malusis, M.A., Shackelford, C.D., 2002. Chemico-osmotic efficiency of a geosynthetic clay liner. J. Geotech. Geoenviron. Eng., ASCE 128 (2), 97–106.

Natsuka, I., Mohri, Y., Asano, I., Yamamoto, S., Miura, N., Fukumoto, S., 1993. The fundamental experiments on the water-proof properties of geosynthetic clay liner using a ultra high pressure mold. Trans. JSIDRE 167, 73–80 (in Japanese).

Saito, A., Chai, J.C., Mizuno, M., 2013. GCL/clayey soil and GM/GCL interface shear strengths and influential factors. Geosynth. Eng. J. 28, 88–92 (in Japanese).

Seo, M.W., Park, J.B., Park, I.J., 2007. Evaluation of interface shear strength between geosynthetics under wet condition. Soils Found. 47 (5), 845–856.

Stark, T.D., Eid, H.T., 1996. Shear behavior of reinforced geosynthetic clay liners. Geosynth. Int. 3 (6), 771–786.

Vukelic, A., Szavits-Nossan, A., Kvasnicka, P., 2008. The influence of bentonite extrusion on shear strength of GCL/geomembrane interface. Geotext. Geomembr. 26 (1), 82–90.

Yamamoto, T., Suzuki, M., Terayama, T., Harada, H., 2001. Evaluation of shear strength along discontinuous planes causing slope failures. Geotech. Eng. Mag. Tsuchi-to-Kiso, Jpn. Geotech. Soc. 49 (7), 7–9 (in Japanese).

Zornberg, J.G., McCartney, J.S., Swan, R.H., 2005. Analysis of a large database of GCL internal shear strength results. J. Geotech. Geoenviron. Eng., ASCE 131 (3), 367–380.